A joint probabilistic index for objective drought identification: the case study of Haiti

Beatrice Monteleone[1], Brunella Bonaccorso[2], and Mario Martina[1]

[1]Scuola Universitaria Superiore IUSS Pavia, Pavia, 27100, Italy
[2]Department of Engineering, University of Messina, S. Agata, Messina, 98166, Italy

Correspondence: Beatrice Monteleone (beatrice.monteleone@iusspavia.it)

Abstract. Since drought is a multifaceted phenomenon, more than one variable should be considered for a proper understanding of such extreme event in order to implement adequate risk mitigation strategies such as weather or agricultural indices insurance programs, or disaster risk financing tools. This paper proposes a new composite drought index that accounts for both meteorological and agricultural drought conditions, by combining in a probabilistic framework two consolidated drought indices: the Standardized Precipitation Index (SPI) and the Vegetation Health Index (VHI). The new index, called Probabilistic Precipitation Vegetation Index (PPVI), is scalable, transferable all over the globe and can be updated in near-real time. Furthermore, it is a remote-sensing product, since precipitation are retrieved from satellite and the VHI is a remote-sensing index. In addition, a set of rules to objectively identify drought events is developed and implemented. Both the index and the set of rules have been applied to Haiti. The performance of PPVI has been evaluated by means of the Receiver Operating Characteristics curve and compared to the ones of SPI and VHI considered separately. The new index outperformed SPI and VHI both in drought identification and characterization, thus revealing potential for an effective implementation within drought early warning systems.

1 Introduction

Droughts affect every year an increasing number of people. In the years from 2014 to 2018 more than 70 drought events have been reported all over the world and about 450 million people suffered because of drought-related impacts (CRED, 2017). Due to its complexity, various definitions of the phenomenon have been proposed by different institutions, such as the World Meteorological Organization (WMO), the Food and Agriculture Organization (FAO) and the United Nations Convention to Combat Desertification (UNCCD). All the institutions focus their attention on a specific aspect of drought: the WMO on the lack of precipitation, the FAO on the decline in crop productivity and the UNCCD on the loss of arable land.

In addition, the quantification of drought effects is a complicated task, since drought impacts are non-structural, widespread over large areas, and of different type and magnitude within the drought-affected area, also depending on economic, social and environmental system vulnerabilities (Wilhite, 2000).

Drought identification through an objective and automatic determination of drought onset, termination and severity allows the timely adoption of appropriate risk management strategies, such as weather index insurance programs (Barnett and Mahul, 2007), agricultural index insurance programs (Jensen and Barrett, 2017), disaster financing (Guimarães Nobre et al., 2019; Linnerooth-Bayer and Hochrainer-Stigler, 2015) and early action planning (Drechsler and Soe, 2016).

Drought features are usually determined through the use of two instruments: indicators, which are variables and parameters used to assess drought conditions (such as precipitation, temperature, and others), and indices, which are numerically computed values from meteorological or hydrological inputs (World Meteorological Organization and Global Water Partnership, 2016). More than 100 indices have been developed by the scientific community (Zargar et al., 2011), each one focusing on a specific aspect of drought (meteorological, hydrological, agricultural and so on). Meteorological drought is related to precipitation shortages; hydrological drought refers to periods of precipitation shortfall on surface water supply (Sheffield and Wood, 2011), while agricultural drought is conventionally linked to soil moisture deficit. Insufficient soil moisture leads to crop failure and consequent yield reduction; therefore the first economic sector suffering because of drought is agriculture, particularly in those areas where it relies on rainfall. A deeper understanding of agricultural drought dynamics can promote the adoption of risk reduction strategies, such as crop insurance programs.

In recent years various remote-sensing indices have been developed and can be employed in agricultural drought monitoring. The most widespread is the Normalized Difference Vegetation Index (NDVI), which uses NOAA AVHRR satellite data to monitor vegetation greenness (Kogan, 1995a). The main advantages of the NDVI are the very high spatial resolution and the global coverage. The NDVI has already been applied in drought monitoring, such as in Gu et al. (2008). Many products were derived from the NDVI, such as the Vegetation Condition Index (VCI), which compares the current NDVI to the range of values observed in the same period in previous years (Liu and Kogan, 1996; Kogan, 1995b) and the Standardized Vegetation Index (SVI), which describes the probability of vegetation condition deviation from normal (Peters et al., 2002). A suite of agricultural drought indices is presented in Table 1.

Since drought is a complex phenomenon, a single index or indicator can be insufficient to fully characterize drought severity and extent. The combination of more than one indicator can be precious to evaluate all the variables involved in drought monitoring, such as precipitation, soil moisture, and streamflow. Over the past 20 years many composite indicators, relying on two or more drought indices or indicators, have been proposed to overcome the issues related to the use of a single variable. Table 2 shows a list of selected composite indices that can be used in agricultural drought monitoring since, in their formulation soil moisture, vegetation condition or variables related to water availability for plants are included.

Multiple methods for taking into account the multivariate behaviour of drought have been explored (Hao and Singh, 2015, 2016). The Vegetation Drought Response Index (VegDRI), for example, uses a data mining approach to combine multiple inputs such as the SPI, the NDVI and the Palmer Drought Severity Index (PDSI). A weighted linear combination of the inputs is quite common; it is applied to construct the Composite Drought Indicator (CDI) for Morocco, the Vegetation Health Index

(VHI) and the Objective Blend of Drought Indicators (OBDI). The United States Drought Monitor (USDM) also applies a weighted linear combination of the inputs but adds an expert judgment to define the drought class.

In the last years multiple studies focused the attention on modelling the joint behaviour of two drought characteristics or indices applying bivariate or multivariate statistical approaches. In various cases bivariate distributions are developed by means of copulas as in Serinaldi et al. (2009) and Bonaccorso et al. (2012), where the joint behaviour of various drought properties is investigated; or in Shiau (2006), where two-dimensional copulas are employed to study the joint behaviour of drought duration and severity in Taiwan. Shiau et al. (2007) investigates also the hydrological droughts of the Yellow River in China using a bivariate distribution to model drought duration and severity jointly. Trivariate Plackett copula is used in Songbai and Singh (2010) to model drought duration, severity and inter-arrival time jointly.

The use of copulas to quantify the joint behaviour of drought indices is gaining popularity too. Many drought indices derived by multivariate distributions have been proposed. For example the Multivariate Standardized Drought Index (MSDI) (Hao and Aghakouchak, 2013), which combines the SPI and the Standardized Soil Moisture Index (SSI), uses copula to form joint probabilities of precipitation and soil moisture content, while the Joint Drought Index (JDI) (Kao and Govindaraju, 2010) does the same for obtaining the joint probabilities while considering precipitation and streamflow. The composite Agrometeorological Drought Index accounting for Seasonality and Autocorrelation (AMDI-SA) combines two drought indices, the Modified SPI, and the Modified SSI, employing both the copula concept and the Kendall function (Bateni et al., 2018). The use of copulas seems promising and is highly effective when dealing with two or more variables. An advantage of copula functions is the fact that the index derived from this approach has a probabilistic form.

Both single and composite indices for agricultural drought monitoring showed some limitations, highlighted in Table 1 and Table 2. Single indices often rely on multiple inputs or are available only for some locations or identify all types of vegetation stresses. In any cases single indices do not account for the multivariate nature of drought. Composite indices often rely on relatively new datasets; in many cases a short period of record is available (for example the VegDri records start in 2009) or the index is not available in near-real time; some of them are specifically designed for a well identified region (the OBDI and the USDM are available only for the USA, the Combined Drought Indicator (CDI) only for Europe); other indices do not consider the meteorological aspect of drought (Temperature Vegetation Index, TVX, and Vegetation Temperature Condition Index, VTCI, are based on the NDVI and the land surface temperature); other ones do not have a sufficiently refined spatial resolution (MSDI). Most of them, with the exception of AMDI-SA and MSDI are not expressed in probabilistic terms, therefore uncertainty quantification and evaluation is not an easy task.

In this paper, we propose:

1. A new drought index, the Probabilistic Precipitation Vegetation Index (PPVI), that takes the advantage of well consolidated indices, the Standardized Precipitation Index (SPI) (Mckee et al., 1993) and the Vegetation Health Index (VHI) (Kogan, 1997) and tries to overcome their individual limitations by coupling them in a probabilistic framework through the use of a bivariate normal distribution function.

2. A framework to identify a drought event using the new index, i.e. a set of rules for the definition of a drought event. When the set of conditions is verified, a drought event is identified based on the new index. Otherwise, no drought event is identified.

With respect to the indices already available in literature, we will show in this paper that the new index has some interesting features:

- it is able to identify drought-driven events of vegetation stress;
- it is parsimonious in terms of number of inputs required;
- it is a remote sensing product with high spatial and temporal resolution;
- it is based on quasi-near real time datasets, with a relatively short latency time (less than one week);
- more than 30 years of records are available at global scale for its calibration.

The paper is structured as follows: Sect.2 describes the datasets employed in the development of the new index and presents the methodology used to combine the SPI and the VHI; Sect. 3 illustrates the application to the case study, shows the validation process of the new index and compares the performance of the new index to those of the SPI and the VHI considered separately; in addition the advantages related to the adoption of the index and the possible applications in agricultural drought risk management are summarized.

2 Datasets and Methods

2.1 Datasets

Two remote-sensing datasets were used: one for precipitation and the other for the VHI. Precipitation was retrieved from the satellite-only Climate Hazard Group Infrared Precipitation (CHIRP) dataset. CHIRP has a quasi-global coverage (50°S - 50°N), high spatial resolution (0.05°) and daily, pentadal and monthly temporal resolution. Records start from 1/1/1981. CHIRP was chosen because it has been specifically developed to monitor agricultural drought. The use of CHIRP instead of CHIRPS (the Climate Hazard Group Infrared Precipitation with Stations) is related to the data latency time. Since the aim of the work is the development of an index for near-real time drought monitoring, the product with the shortest latency time was selected. CHIRPS data have a latency time of about three weeks (Funk et al., 2015), while CHIRP's latency is about 2 days, as can be checked on the dataset website (Climate Hazard Group, 2015). The development and the main characteristics of the dataset are described in Funk et al. (2015). In the present study CHIRP with a daily temporal resolution was used to have the possibility to compute weekly precipitation. Data are available on the project website (Climate Hazard Group, 1999).

The Vegetation Health Index was retrieved from the Global Vegetation Health Products (Global VHP) of the National Oceanic and Atmospheric Administration Center of Satellite Applications and Research (Kogan, 1997). Data can be retrieved at the NOAA website (NOAA, 2011). The dataset contains Blended-VHP derived from VIIRS (2013-present) and AVHRR

(1981-2012) GAC data. The dataset has $4\mathrm{km}$ spatial resolution, weekly temporal resolution, and global coverage. Both the selected datasets are freely available.

2.2 Methods

2.2.1 The Standardized Precipitation Index

As previously mentioned, two consolidate drought indices were combined: the SPI and the VHI. The SPI was selected because it is a commonly used index to detect meteorological drought, it is standardized, therefore SPI values can be compared even in different climate regimes and it is recommended by the WMO (World Meteorological Organization, 2009).

SPI computation is based on a long-term precipitation record for a desired period. The precipitation record is then fitted to a probability distribution (in this work a gamma distribution was used), which is then transformed into a normal distribution. Traditionally monthly precipitation records are employed, and SPI is computed aggregating precipitation at a predefined timestep (for example 1 month, 3 months, 6 months, 9 months and 12 months are the aggregation periods suggested by the WMO (World Meteorological Organization, 2009)).

In the present work, weekly precipitation records were used. The SPI aggregation period was then selected and the index, computed over one of the the traditional aggregation periods, was updated every week. SPI is normal distributed by definition. Conventionally drought starts when SPI is lower than -1 and ends when SPI comes back to the value of 0 (Mckee et al., 1993). Drought classification according to SPI, as proposed in Mckee et al. (1993), is reported in Table 3. The percentages reported in the third column of Table 3 indicate the probability for SPI values to fall within the range reported in the second column of the same table.

2.2.2 The Vegetation Health Index

The VHI is a remote-sensing index developed to include the effects of temperature on vegetation; in fact, it combines the VCI with the Temperature Condition Index (TCI) (Kogan, 1995a), which is another remote-sensing index used to determine vegetation stress caused by temperature and excessive wetness. The VHI is based on a linear combination of VCI and TCI, $VHI = \alpha VCI + (1-\alpha)TCI$. As suggested by Kogan et al. (2016), when VCI and TCI contributions are not known $\alpha = 0.5$. One drawback of the VHI is the impossibility to identify the cause of the vegetation stress; in fact, vegetation can suffer because of various events: excessive wetness, pests, fires, droughts or others. It is a biophysical indicator of a lack of precipitation but can also be seen as representing drought impacts on the ground (Bachmair et al., 2016). It goes from 0, which stands for vegetation in very bad conditions to 100, meaning perfectly healthy vegetation. The classification scheme of VHI, as proposed in Dalezios et al. (2017), is presented in Table 4.

The VHI is standardized to make comparisons with the SPI easier. As mentioned by Peters et al. (2002), all remote-sensing indices can be expressed as deviations from the mean; therefore, the standardized variable, VHI_{st}, is computed according to

the following equation:

$$VHI_{st} = \frac{VHI - \overline{VHI}}{\sigma} \tag{1}$$

where $\overline{VHI}$ is the mean of the distribution and σ its standard deviation. Thus, the same procedure proposed in Peters et al. (2002) in the case of the NDVI has been applied to the VHI. The standardized variable, VHI_{st}, has a distribution with 0 mean and 1 as standard deviation.

2.2.3 The Probabilistic Precipitation Vegetation Index (PPVI)

The Probabilistic Precipitation Vegetation Index (PPVI) is a composite index that takes into account both meteorological drought through the SPI, and agricultural drought conditions by including the VHI.

In order to combine the two consolidated indices the following preparatory steps are performed:

1. Extraction of the area under study from both the datasets;
2. Regridding of both precipitation and the VHI to bring them to the same spatial resolution (0,05°);
3. Aggregation of precipitation at weekly timescale (CHIRP has daily temporal resolution);
4. Computation and weekly update of SPI according to the methodology proposed in USDA Risk Management Agency et al. (2006), where precipitation are fitted to a gamma distribution. The goodness of fit to the gamma distribution has been verified by means of probability plot.
5. Standardization of the VHI, as previously described.

The combination of SPI and VHI is performed using a bivariate normal distribution function, as it is defined by Kotz et al. (2000). The normality of the SPI and VHI_{st} distributions has been verified as will be shown in Sect. 3.2. Therefore it is acceptable to assume that the joint probability of the two considered distributions takes the form of the bivariate normal for correlated variables:

$$f(s,v) = \frac{1}{2\pi\sigma_s\sigma_v\sqrt{1-\rho^2}} \exp\left(-\frac{1}{2(1-\rho^2)}\left[\frac{(s-\mu_s)^2}{\sigma_s} + \frac{(v-\mu_v)^2}{\sigma_v} + \frac{2\rho(s-\mu_s)(v-\mu_v)}{\sigma_s\sigma_v}\right]\right) \tag{2}$$

where the following notation is adopted: the *SPI* is identified as *s* and the VHI_{st} is identified as *v*. The mean and the standard deviation of the SPI distribution $f(s)$ are respectively, by construction, $\mu_s = 0$ and $\sigma_s = 1$ and the mean and standard deviation of the VHI_{st} distribution, $f(v)$ are respectively $\mu_v = 0$ and $\sigma_v = 1$. The covariance matrix Σ and the correlation coefficient ρ are defined according to Eqs. 3 and 4 respectively, where σ_{sv} is the covariance between *s* and *v*.

$$\Sigma = \begin{bmatrix} \sigma_s^2 & \rho\sigma_s\sigma_v \\ \rho\sigma_s\sigma_v & \sigma_v^2 \end{bmatrix} \tag{3}$$

$$\rho = \frac{\sigma_{sv}}{\sigma_s \sigma_v} \tag{4}$$

To check the assumption of normality for the joint distribution, the joint probability values, retrieved from Eq.2 are plotted against the bivariate empirical cumulative distribution values (Fig.1), as done in (Kao and Govindaraju, 2010). The bivariate empirical copula for the random variables *s* and *v* has been evaluated according to Nelsen (2006) using the following equation:

$$C\left(\frac{i}{m}, \frac{j}{m}\right) = \frac{\#(s \leq s_{(i)}, v \leq v_{(j)})}{m} = \frac{m_1}{m} \tag{5}$$

where $s_{(i)}$ and $v_{(j)}$, $(1 \leq i, j \leq m)$ are ordered statistics of the ***SPI*** sample of size m, m_1 is the number of samples $(s_{(k)}, v_{(k)})$ satisfying $(s_{(k)} \leq s_{(i)}\ and\ v_{(k)} \leq v_{(j)})$ with $1 \leq k \leq m$. The resulting plot is shown in Fig.1.

Since the data lays on the 45°line it is fair to assume that the joint probability $f(s, v)$ is normal. Therefore, a normalization of the index is performed through normal quantile transformation.

By keeping the same probability intervals of the SPI, we can compute the PPVI values for the drought classification as it is shown in Table 5.

2.2.4 Identification of drought events

Once the index is defined the set of rules to establish when a grid cell is in drought should be identified. In particular, two parameters have to be identified:

1. A threshold *Z* of the index that marks the beginning of a drought in a grid cell.
2. A threshold *z* that marks the end of a drought in the same grid cell.

According to the model here proposed a drought in a grid cell starts when the index is lower than *Z* and ends when the index is above to *z*. Then regional drought events are defined. Again, two parameters are identified: *N* and *n*. A drought events starts if more than *N* grid cells are in drought conditions and ends if less than *n* grid cells are in drought conditions.

2.2.5 Skill assessment

Observations of drought are compared with the model outputs for various combinations of thresholds *Z*, *z*, *N* and *n*. The Receiver Operating Characteristic (ROC) curve is used for this comparison. The ROC curve was at first used in signal detection; its use in meteorological applications is documented and well described in Joliffe and Stephenson (2012). The ROC curve is employed to classify instances, as in the present case. The ROC curve was already employed in various studies to compare the performance of a model versus observations with varying thresholds (Zhu et al., 2016; Khadr, 2016). The contingency matrix (shown in Table 6) is a two by two matrix to visualize the disposition of a set of instances. True positive or hits are represented by the weeks that are reported to be in drought conditions in the observations and are correctly identified as drought weeks

by the model. True negatives (correct rejections) are represented by those weeks that are not in drought according to both the observations and the model. Those weeks that are recorded as drought according to the observations but are not identified as drought weeks by the model, are considered as false negatives (missing events), while false positives (false alarms) are represented by the weeks that are not in drought conditions according to the observations but are identified as drought weeks by the model. In this paper for each combination of thresholds *Z*, *z*, *N* and *n*, Probability of Detection (POD), or hit rate, and Probability of False Detection (POFD), or false alarm rate, are computed according to Joliffe and Stephenson (2012) with the following equations:

$$POD = \frac{TP}{TP + FN} \tag{6}$$

$$POFD = \frac{TN}{TN + FP} \tag{7}$$

where *TP*,*TN*,*FP* and *FN* are defined as in Table 6.

The optimal threshold for a ROC curve is the one for which the distance from the 45°degree line is maximum (Zhu et al., 2016). The performances of the model based on PPVI in identifying drought events have been evaluated on the case study described in the next section.

2.2.6 Case study

The case study region is Haiti. The country, which has an extension of 27.750 km^2 is located in the Caribbean's Great Antilles and shares the island of Hispaniola with the Dominican Republic. The climate is predominantly tropical, with daily temperatures ranging between 19°C and 28°C during winter and between 23°C and 33°C during summer. The island topography is varied; the central region is mainly mountainous, while the northern and western regions are near the coastline. Annual precipitation in the central region averages 1.200 mm, while in the lowlands it is about 550 mm (GFDRR, 2011). Haiti is subject to the variability associated with El Niño and La Niña phenomena, with El Niño bringing drier and hotter conditions and La Niña colder and wetter climate. Haiti experiences a first rainy season from April to July and a second, and most important, from August to the end of November. The dry season starts in December and goes on until the end of March (FEWSNET, 2019).

Haiti is divided administratively into 10 departments (Fig. 2), with people living mainly in the West, where the capital Port-au-Prince is located, and in the Artibonite. The total population in 2017 was about 11 million people (World Bank, 2017). Haiti is the poorest country in the Western Hemisphere, the economy is mainly agricultural. 67% of the country's area is devoted to agriculture, but only 4,35% of the agricultural area is irrigated (Trading Economics, 2013), posing a major threat to local production.

Haiti produces over half of the world's vetiver oil (used in cosmetics), and mangos and cocoa are the most important export crops. Two-fifths of all Haitians depend on the agriculture sector, mainly small-scale subsistence farming. The country is prone to all types of natural hazards. Earthquakes, storms, hurricanes, landslides, and droughts have caused huge damages and losses

in recent years. Haiti was ranked as the third most affected country by extreme weather events in terms of lives lost and economic damages in the period from 1994 to 2013 (GFDRR, 2011). More than 96% of the population lives in areas at risk of two or more hazards. The most frequent disasters are floods and storms but, when considering the number of affected people, droughts are the disasters involving the highest number of persons (Fig. 3).

Droughts threat the livelihoods of Haitians in many different ways. The scarcity of crops production means a rise in food prices, that brings to widespread food insecurity since the major part of people can't afford the increase. Unavailability of drinking water leads to cholera outbreaks among the population. Water is an issue also for breeders, who lose livestock on which they rely for milk production and meat consumption. In the period from 1980 to present more than 10 drought events have been reported by the government or the humanitarian organizations working in Haiti (Table 7). The worst drought was the one of 2014-2017, affecting more than 3 million inhabitants (about one-third of Haiti's population).

Effective drought management is crucial for Haiti, but at present, a reliable early warning system for drought is still lacking. Weather stations on the ground are few and data records are often very short, therefore not useful for drought monitoring purposes on the entire country. Satellite images can be an effective and not expensive way to improve drought management and preparedness in the country.

3 Results and Discussion

3.1 Correlation analysis

Haiti has been divided into 987 grid cells, accounting for 90% of the country area. 1941 weeks were considered, starting from week 35 of 1981 and ending with week 52 of 2018. The release date of a new VHI image was considered as the starting date for a week. In the present study, four precipitation aggregation periods were considered (1 months, 2 months, 3 months and 6 months) and the corresponding values of SPI (SPI1, SPI2, SPI3 and SPI6) were computed in order to select the SPI aggregation timescale to be used to create the PPVI.

To evaluate the strength of the statistical relationship between the SPI at various timescales and the VHI a correlation analysis was then performed. Various studies have already evaluated the correlation among drought indices or between drought indices and exogenous variables; for example (Bonaccorso et al., 2015) investigated the correlation between SPI and North Atlantic Oscillation (NAO), while Hongshuo et al. (2014) investigated the correlation between SPI (various aggregation periods) and the VHI. The Pearson correlation coefficient was employed in the present study as a measure of the statistical relationship between the indices. The number of significant correlations at 5% and 1% was evaluated for four SPI aggregation timescales (Table 8). The highest number of significant correlations was found in the cases of SPI2 and SPI3, which exhibit very similar performances at 1% significant level. This finding is in agreement with previous studies such as Hongshuo et al. (2014) that found that VHI and SPI3 have the highest correlation for croplands, whereas VHI and 6-month SPI have the highest correlation for forest in the Southwest of China; and Ma'rufah et al. (2017) that found that significant correlation coefficient values on SPI3 and VHI are common in the southern part of Indonesia. Since SPI3 has been used in literature and the percentage of

significant correlation at 1% level is relevant, it has been decided to aggregate SPI over a 3 months period and use SPI3 in the following discussion.

3.2 Normality of SPI and VHI distributions

Before computing PPVI as described in the previous sections, a test on the normality of the SPI3 and VHI_{st} distributions was performed. The goodness of fit of the SPI3 and the VHI_{st} distributions was verified through the histograms in Fig. 4 (panel (a) and (b) respectively), where the boxplots represent the relative frequencies of the SPI3 and VHI_{st} values. Both the SPI3 and the VHI_{st} data can therefore be considered normally distributed.

3.3 Selection of threshold values

PPVI was computed as described in Sect. 2.2 and its performance in identifying past drought events in Haiti when used in combination with the set of rules described in Sect. 2.2.4 was evaluated. To this end, the ROC curve classification methodology was applied. The set of rules implied that at first, cells in drought conditions were identified: drought started in a specific grid cell at week *W* when PPVI was lower than the threshold *Z* and ended when PPVI was up to the threshold *z* in the same grid cell at a week *w* (with *w* coming after *W*). Then a regional drought event was identified: the drought event started when more than *N* cells at a specific week W_1 were in drought conditions and ended at a week W_2 when few than *n* grid cells were in drought conditions. The comparison was performed on a weekly basis, with observations derived from the reported events described in Table 7.

The ROC curves were computed according to the following methodology: at first a combination of the thresholds *Z*, *z*, *N* and *n* was selected. On the basis of the set of rules established in Sect. 2.2.4, the ability of the selected combination of thresholds in reproducing the observations was assessed by computing *TP*, *TN*, *FP* and *FN* as defined in Table 6, together with POD and POFD. A couple (POFD, POD) represents a point in a ROC graph. Then one threshold among *Z*, *z*, *N* and *n* was selected. The selected threshold was variable during the analysis, while the other three were kept constant. The step of variation was identified according to the threshold maximum and minimum values. For each combination of the four thresholds (the varying one and the three fixed) *TP*, *TN*, *FP*, *FN* and POD and POFD were computed. The resulting set of couples (POFD, POD) represented the ROC curve for the considered set of thresholds.

The analysis was repeated by varying another threshold among *Z*, *z*, *N* and *n*. As an example, Fig. 5 shows four ROC curves for the thresholds in Table 9. Thresholds *N* and *n* in Table 9 are expressed as the percentage of the country's area instead as the number of grid cells. For each of the curves the best performing set of (*Z*, *z*, *N* and *n*) was selected by identifying the point farther from the 45°line, as done by Zhu et al. (2016). The Area Under the Curve (AUC) was used as criteria to establish which of the ROC curves should be preferred (as was done by Dutra et al. (2014); Mason and Graham (2002); Zhu et al. (2012)). An AUC near to 1 indicates good performance, while AUC of 0.5 indicates the model has no predictive skills. From Fig. 5 it is clear that the curve corresponding to the parameters defined as "Set 2" in Table 9 should be preferred, since the AUC is the closest to 1.

3.4 Comparison of drought indices with observed drought events

The aim of this paragraph is not to validate in absolute terms the proposed methodology since the data record is too short to serve both for calibration and for validation. In the present section, instead, we provide a validation by comparing the performance of PPVI in identifying observed drought events with the one of widely recognized and used indices such as SPI and VHI.

The performance of PPVI was then compared to the one of SPI3 and VHI considered separately. Thresholds analogous to *Z* and *z* were defined for SPI3 and VHI. Thresholds Z_S and z_S mark respectively the beginning and the end of drought conditions in a grid cell according to SPI3 and thresholds Z_V and z_V do the same in the case of VHI. Again the four thresholds *Z*, *z*, *N*, and *n* were varied in order to identify the optimal values. As an example Fig. 6 shows a comparison among the ROC curves for the three indices. In each panel of Fig. 6, *n* and *z*, z_S and z_V (for PPVI, SPI3 and VHI) remained constant, while *Z*, Z_S and Z_V were varying; *N* was fixed in each panel but varied among the panels. *Z* varied from -4 to -1.1 with a step equals to 0.1; Z_S varied from -3 to 0 with a step equals to 0.1 and Z_V varied from 10 to 40 with a step equal to 5.

It is clear from Fig. 6 that the red curve, representing PPVI, is the furthest from the diagonal line in all the panels of the figure. The Area Under the Curve (AUC) was used as criteria to establish which index gave the best performances. AUC values are shown in Fig. 6 for each index and various configurations of the model. The AUC value of PPVI was in line with similar results reported in literature (Mwangi et al., 2014). As can be seen from Fig. 6, the new index provided better results with respect to the ones obtained with SPI3 or VHI considered separately. In all the four configurations shown in Fig. 6, the AUC for the curve constructed with PPVI was higher than the ones for SPI3 and VHI. The AUC values are in line with the ones considered good in the literature (see Khadr (2016)) for drought predictive skills. The optimal thresholds to configure the model when applied with each of the three considered indices were then determined by selecting the point farther from the 45°line, as done by Zhu et al. (2016). The best configurations parameters are shown in Table 10. The drought events were therefore identified using the optimal parameters (Table 10). A graphical representation of the performance of the model in reproducing observed drought events is given in Fig. 7. Only the period from 2000 to 2018 is shown.

The ability of the model in identifying the country area hit by the drought was also assessed. A visual comparison among the area under drought identified by the three indices was performed, as was done by Dutta et al. (2015).

Here some significant weeks are shown. At first, week 45 of 1995 was considered. No drought events were reported in that period according to the information available in the analysed documents (see Table 7). Figure 8 shows that, while SPI3 identified all the southern part of the country as dry areas and VHI showed vegetation suffering in two departments (Centre and West), PPVI did not show signs of drought, except for a minor number of grid cells. Figure 9 shows that in 2015, when the whole country was reported to be in severe drought conditions (see Table 7 and NOAA (2017); OXFAM and Action contre la Faim (2015)), PPVI captured well the pattern, only a few grid cells were not in drought conditions. The SPI3 was also able to catch the situation, while for the VHI only 58% of the county was in drought. During week 8 of 2012, only the Northern part of the country was in drought (Fig. 10), as highlighted by USAID and FEWSNET (2012b) (see Table 7). Five departments were reported to be stressed (North, North West, North East, Artibonite, Centre, see Table 7). All the three indices showed the North

West as the department most affected by drought when considering the percentage of the department area hit by the drought. PPVI then classified Artibonite, North, Centre and North East, while SPI3 as second and third most affected departments identified South and Grand Anse and VHI Centre and Nippes (Table 11).

Severity, duration and mean areal extent of the drought events identified by PPVI were computed. Severity was computed as the sum of all the values identified by the condition that a grid cell is in a drought condition when PPVI is lower than -1.8 and exits from drought when PPVI is up to -1.1. Duration is expressed in months and the mean areal extent is the average percentage of area in drought during a specific event. Results are presented in Table 12.

PPVI showed overall a better capacity in identifying drought events with respect to SPI3 and VHI considered separately. However, some false alarms still remain. This can be linked to the uncertainty in information on past drought events for the analysed area. Short-term droughts are often not reported in text-based documents, and information on drought start and end date were retrieved from documents that mainly described the impacts related to drought. PPVI showed a good agreement with reported information in identifying the areas of the country hit by the drought.

4 Conclusions

The timely identification of drought events is of great importance in agricultural areas, especially when rainfed agriculture is practiced. At the same time, the evaluation of the damages caused by drought is a key point to select appropriate risk management strategies, such as weather index insurance programs, agricultural index insurance, disaster financing and early action planning. The new composite index proposed in this paper, the Probabilistic Precipitation Vegetation Index, PPVI, is a powerful tool since it can identify events of vegetation stress, and at the same time, select among those the ones actually due to drought, thanks to the contemporary use of both VHI and SPI. As such it can be helpful in agricultural drought monitoring and can be used to identify drought events affecting a region, their severity and their duration as was shown in the case of Haiti. In particular, PPVI can be precious in those areas where rainfed agriculture is of vital importance since people rely on it for food production for personal consumption.

Among the interesting aspects of PPVI, there is the fact that few data are required for its computation: only precipitation and the VHI. This aspect is crucial, since many composite indicators able to identify agricultural droughts already exist, but large amounts of data are required to compute them. For example, the United States Drought Monitor combines more than 40-50 inputs, while other indices specific for agricultural drought monitoring, such as the VegDRI and the VegOut, require the use of temperature and oceanic indices. The number of parameters required to compute PPVI is lower even with respect to OBDI, SWS, CDI or CDSI.

A second most important advantage is that, since the SPI was computed starting from satellite precipitation (CHIRP dataset) and that the VHI is a remote-sensing drought index, PPVI is also a remote-sensing product. The use of datasets with global coverage means that PPVI is easily transferable and scalable over the entire globe. In addition, PPVI can be a very useful tool in areas with scarce gauge coverage as the Caribbean Islands. Both precipitation and the VHI have a very high spatial and temporal resolution, thus allowing drought monitoring from satellite even in small areas. PPVI can be computed even in those

regions with short data records, since the VHI has more than 30 years of records (data collection began in August 1981); and CHIRP precipitation are available from January 1981.

Both the SPI and the VHI are updated at weekly time-step since every week a new VHI image is released and the CHIRP precipitation dataset has a daily temporal resolution, therefore PPVI can be updated more frequently than other composite indices, such as CDI, which is updated every 10 days. In addition, due to the relatively short latency time (less than one week) of both the datasets employed to create PPVI, the index is available in near-real time, therefore allows the timely implementation of drought mitigation strategies. This last feature is of particular interest when PPVI is used to implement measure to reduce drought risk in agriculture, where a timely identification of drought is crucial to prevent damages to the sector.

Many advantages are also related to the adoption of the set of rules here proposed to identify drought events. First of all, these rules enable an objective and standardized identification of drought events from the mathematical point of view. Additionally, they can be adjusted according to the needs and the objectives of various possible end users of the model, such as farmers, governments or insurance companies.

The performances of PPVI in identifying drought events were tested in a specific case study (Haiti) and compared to the ones of SPI and VHI considered separately. PPVI performed better than the single indices considered separately in reproducing past drought events. PPVI identified drought areas in Haiti better than SPI and VHI even from the spatial point of view, thus it is more reliable than a single index. A comparison of PPVI performances with respect to the ones of other composite indices was not performed in the present study due to the unavailability of composite indices with the same characteristics of PPVI. In fact previous composite indices do not include both the meteorological and the agricultural aspect of drought or are not available globally, or cannot be computed with only remote sensing datasets.

Author contributions. This research is part of the PhD thesis from BM. BB and MM were both the thesis supervisors.

Competing interests. The authors declare that they have no conflict of interest.

Acknowledgements. The research leading to these results has received funding from the Disaster Risk Financing Challenge Fund of the World Bank Group in the context of the SMART (A Statistical Machine Learning Framework for Parametric Risk Transfer) project. The research has been developed within the framework of the project 'Dipartimenti di Eccellenza', funded by the Italian Ministry of Education, University and Research at IUSS Pavia.

References

Bachmair, S., Stahl, K., Collins, K., Hannaford, J., Acreman, M., Svoboda, M., Knutson, C., Smith, K. H., Wall, N., Fuchs, B., Crossman, N. D., and Overton, I. C.: Drought indicators revisited: the need for a wider consideration of environment and society, Wiley Interdisciplinary Reviews: Water, 3, 516–536, https://doi.org/10.1002/wat2.1154, http://doi.wiley.com/10.1002/wat2.1154, 2016.

Barnett, B. J. and Mahul, O.: Weather Index Insurance for Agriculture and Rural Areas in Lower-Income Countries, American Journal of Agricultural Economics, 89, 1241–1247, 2007.

Bateni, M., Behmanesh, J., and Bazrafshan, J.: Composite Agrometeorological Drought Index Accounting for Seasonality and Autocorrelation, Journal of Hydrologic Engineering, 23, https://doi.org/10.1061/(ASCE)HE.1943-5584.0001654, 2018.

BC Ministry for Agriculture: Soil water storage capacity and available soil moisture, Tech. rep., 2015.

Bergman, K., Sabol, P., and Miskus, D.: Experimental Indices for monitoring global drought conditions, Proceedings of 13th Annual Climate Diagnostics Workshop,, 1988.

Bijaber, N., Hadani, D. E., Saidi, M., Svoboda, M. D., Wardlow, B. D., Hain, C. R., Poulsen, C. C., Yessef, M., and Rochdi, A.: Developing a Remotely Sensed Drought Monitoring Indicator for Morocco, Geosciences, 8, 1–18, https://doi.org/10.3390/geosciences8020055, 2018.

Bonaccorso, B., Cancelliere, A., and Rossi, G.: Methods for Drought Analysis and Forecasting, in: Handbook of Methods and Applications of Statistics in the Atmospheric and Earth Sciences, pp. 150–184, 2012.

Bonaccorso, B., Cancelliere, A., and Rossi, G.: Probabilistic forecasting of drought class transitions in Sicily (Italy) using Standardized Precipitation Index and North Atlantic Oscillation Index, Journal of Hydrology, 526, 136–150, https://doi.org/10.1016/j.jhydrol.2015.01.070, http://dx.doi.org/10.1016/j.jhydrol.2015.01.070, 2015.

Brown, J. F., Wardlow, B. D., Tadesse, T., and Hayes, M. J.: The Vegetation Drought Response Index (VegDRI): A New Integrated Approach for Monitoring Drought Stress in Vegetation, GIScience & Remote Sensing, 45, https://doi.org/10.2747/1548-1603.45.1.16, 2008.

CIAT: Atlas des menaces naturelles en Haiti, Tech. rep., http://ciat.gouv.ht/articles/atlas-des-menaces-naturelles-en-haiti, 2017.

Climate Hazard Group: Climate Hazard Group InfraRed Precipitation data archive, ftp://ftp.chg.ucsb.edu/pub/org/chg/products/CHIRP/, 1999.

Climate Hazard Group: Chirp daily, ftp://ftp.chg.ucsb.edu/pub/org/chg/products/CHIRP/daily/, 2015.

CNSA/MARNDR and FEWSNET: Haiti Food Security Update September 2009, https://reliefweb.int/report/haiti/haiti-food-security-update-april-september-2009, 2009.

CRED: EM-DAT The International Disaster Database, http://emdat.be/emdat{_}db/, 2017.

Dalezios, N. R., Tarquis, A. M., and Eslamian, S.: Droughts, in: Environmental Hazards Methodologies for Risk Assessment and Management, edited by Dalezios, N. R., chap. 5, IWA Publishing, https://doi.org/10.2166/9781780407135, 2017.

Dieker, E., van Lanen, H. A. J., and Svoboda, M.: Comparison of three drought monitoring tools in the USA, Tech. Rep. 25, 2010.

Drechsler, M. and Soe, W.: Early Warning , Early Action The Use of Predictive Tools in Drought Response through Ethiopia ' s Productive Safety Net Programme, Tech. Rep. June, World Bank, 2016.

Dutra, E., Pozzi, W., Wetterhall, F., Giuseppe, F. D., Magnusson, L., Naumann, G., Barbosa, P., and Vogt, J.: Global meteorological drought – Part 2 : Seasonal forecasts, Hydrology and Earth System Sciences, 18, 2669–2678, https://doi.org/10.5194/hess-18-2669-2014, 2014.

Dutta, D., Kundu, A., Patel, N., Saha, S., and Iddiqui, A.: Assessment of agricultural drought in Rajasthan (India) using remote sensing derived Vegetation Condition Index (VCI) and Standardized Precipitation Index (SPI), The Egyptian Journal of Remote Sensing and Space Sciences, 18, 53–63, https://doi.org/10.1016/j.ejrs.2015.03.006, 2015.

FEWSNET: HAITI Food Security Outlook Update May 2013, Tech. Rep. May, https://reliefweb.int/report/haiti/haiti-food-security-outlook-update-may-2013, 2013.

FEWSNET: Haiti seasonal calendar, http://fews.net/central-america-and-caribbean/haiti, 2019.

Funk, C., Peterson, P., Landsfeld, M., Pedreros, D., Verdin, J., Shukla, S., Husak, G., Rowland, J., Harrison, L., Hoell, A., and Michaelsen, J.: The climate hazards infrared precipitation with stations - A new environmental record for monitoring extremes, Scientific Data, 2, 1–21, https://doi.org/10.1038/sdata.2015.66, 2015.

GFDRR: Climate Risk and Adaptation Country Profile: vulnerability, risk reduction and adaptation to climate change in Haiti, Tech. Rep. April, 2011.

Gu, Y., Hunt, E., Wardlow, B., Basara, J. B., Brown, J. F., and Verdin, J. P.: Evaluation of MODIS NDVI and NDWI for vegetation drought monitoring using Oklahoma Mesonet soil moisture data, Geophysical Research Letters, 35, 1–5, https://doi.org/10.1029/2008GL035772, 2008.

Guimarães Nobre, G., Davenport, F., Bischiniotis, K., Veldkamp, T., Jongman, B., Funk, C. C., Husak, G., Ward, P. J., and Aerts, J. C. J. H.: Financing agricultural drought risk through ex-ante cash transfers, Science of the Total Environment, 653, 523–535, https://doi.org/10.1016/j.scitotenv.2018.10.406, https://doi.org/10.1016/j.scitotenv.2018.10.406, 2019.

Hao, Z. and Aghakouchak, A.: Advanc es in Water Resou rces Multivariate Standardized Drought Index : A parametric multi-index model, Advances in Water Resources, 57, 12–18, https://doi.org/10.1016/j.advwatres.2013.03.009, http://dx.doi.org/10.1016/j.advwatres.2013.03.009, 2013.

Hao, Z. and Singh, V.: Review of dependence modeling in hydrology and water resources, Progress in Physical Geography, 40, 549–578, https://doi.org/10.1177/0309133316632460, 2016.

Hao, Z. and Singh, V. P.: Drought characterization from a multivariate perspective : A review, Journal of Hydrology, 527, 668–678, https://doi.org/10.1016/j.jhydrol.2015.05.031, http://dx.doi.org/10.1016/j.jhydrol.2015.05.031, 2015.

Hongshuo, W., Hui, L., and Desheng, L.: Remotely sensed drought index and its responses to meteorological drought in Southwest China, Remote Sensing Letters, 5, 2014.

Idso, S., Jackson, R., Pinter, P. J., Reginato, R., and Hatfield, J.: Normalizing the stress-degree-day parameter for environmental variability, Agricultural Meteorology, 24, 1981.

Jensen, N. and Barrett, C.: Agricultural Index Insurance for Development, Applied Economic Perspectives and Policy, 39, 199–219, https://doi.org/10.1093/aepp/ppw022, 2017.

Joliffe, I. T. and Stephenson, D. B.: Forecast Verification: a practitioner's guide in Atmospheric Science, https://doi.org/10.1016/B978-0-12-385022-5.00008-7, 2012.

Kao, S.-c. and Govindaraju, R. S.: A copula-based joint deficit index for droughts, Journal of Hydrology, 380, 121–134, https://doi.org/10.1016/j.jhydrol.2009.10.029, http://dx.doi.org/10.1016/j.jhydrol.2009.10.029, 2010.

Karamouz, M., Rasouli, K., and Nazif, S.: Development of a Hybrid Index for Drought Prediction : Case Study, Journal of Hydrologic Engineering, 14, 617–627, 2009.

Keyantash, J. and Dracup, J.: An aggregate drought index: Assessing drought severity based on fluctuations in the hydrologic cycle and surface water storage, Water Resources Research, 40, 2004.

Khadr, M.: Forecasting of meteorological drought using Hidden Markov Model (case study : The upper Blue Nile river basin , Ethiopia), Ain Shams Engineering Journal, 7, 47–56, https://doi.org/10.1016/j.asej.2015.11.005, http://dx.doi.org/10.1016/j.asej.2015.11.005, 2016.

Kogan, F. N.: Remote sensing of weather impacts on vegetation in non-homogeneous areas, International Journal of Remote Sensing, 11, 1405–1419, 1990.

Kogan, F. N.: Droughts of the late 1980s in the United States as derived from NOAA polarorbiting satellite data, Bulletin of the American Meteorology Society, 76, 655–668, 1995a.

Kogan, F. N.: Application of vegetation index and brightness temperature for drought detection, Advances in Space Research, 15, 2761–2782, 1995b.

Kogan, F. N.: Global Drought Watch from Space, Bulletin of the American Meteorological Society, 78, 621–636, 1997.

Kogan, F. N., Guo, W., Strashnaia, A., A., K., Chub, O., and Virchenko, O.: Modelling and prediction of crop losses from NOAA polar-orbiting operational satellites, Geomatics, Natural Hazards and Risk, 7, 886–900, https://doi.org/10.1080/19475705.2015.1009178, 2016.

Kotz, S., Balakrishnan, N., and Johnson, N. L.: Continuous Multivariate Distributions, John Wiley & Sons, second edi edn., https://doi.org/10.1002/0471722065, 2000.

Lambin, E. and Ehrlich, D.: Combining vegetation indices and surface temperature for land-cover mapping at broad spatial scales, International Journal of Remote Sensing, 16, 1995.

Linnerooth-Bayer, J. and Hochrainer-Stigler, S.: Financial instruments for disaster risk management and climate change adaptation, Climatic Change, 133, 2015.

Liu, W. and Kogan, F. N.: Monitoring regional drought using the Vegetation Condition Index, International Journal of Remote Sensing, 17, 2761–2782, 1996.

Ma'rufah, U., Hidayat, R., and Prasati, I.: Analysis of relationship between meteorological and agricultural drought using standardized precipitation index and vegetation health index, in: Earth and Environmental Science, vol. 54, p. 7, https://doi.org/10.1088/1742-6596/755/1/011001, 2017.

Mason, S. and Graham, N.: Area beneath the relative operating characteristics (ROC) and relative operating levels (ROL) curves: statistical significance and interpretation, Quarterly Journal of the Royal Meteorological Society, 128, 2145–2166, https://doi.org/10.1016/B978-1-4377-0795-3.00025-9, 2002.

Matera, A., Fontana, G., and Marletto, V.: Use Of a New Agricultural Drought Index Within a Regional Drought Observatory, in: Methods and Tools for Drought Analysis and Management, edited by Rossi, G., pp. 103–124, Springer, 2007.

Mckee, T. B., Doesken, N. J., and Kleist, J.: The relationship of drought frequency and duration to time scales, in: AMS 8th Conference on Applied Climatology, January, pp. 179–184, https://doi.org/10490403, http://ccc.atmos.colostate.edu/relationshipofdroughtfrequency.pdf, 1993.

Meyer, S. J., Hubbard, K. G., and Wilhite, D. A.: Crop-Specific Drought Index for Corn: I. Model Development and Validation, Agronomy Journal, 86, 388–395, https://doi.org/10.2134/agronj1993.00021962008500020040x, 1993.

Mora-Castro, S.: Personal communication.

Mora-Castro, S.: Etude de reconaissance sur les differents types des menaces naturelles dans le basin versant de l'Artibonite, Haiti, Tech. rep., Ingeosa, Port au Prince, 1986.

Mwangi, E., Wetterhall, F., Dutra, E., Di Giuseppe, F., and Pappenberger, F.: Forecasting droughts in East Africa, Hydrology and Earth System Sciences, 18, 611–620, https://doi.org/10.5194/hess-18-611-2014, 2014.

Narasimhan, B. and Srinivasan, R.: Development and evaluation of Soil Moisture Deficit Index (SMDI) and Evapotranspiration Deficit Index (ETDI) for agricultural drought monitoring, Agricultural and Forest Meteorology, 133, 69–88, https://doi.org/10.1016/j.agrformet.2005.07.012, 2005.

Nelsen, R. B.: An Introduction to Copulas, Springer-Verlag, New York, 2 edn., https://doi.org/10.1007/0-387-28678-0, 2006.

NOAA: STAR—Global Vegetation Health Products. National Oceanic and Atmospheric Administration (NOAA), https://www.star.nesdis.noaa.gov/smcd/emb/vci/VH/vh{_}ftp.php, 2011.

NOAA: Climate Prediction Center ' s Hispaniola Hazards Outlook: October 5- October 11, 2017, Tech. rep., NOAA, 2017.

NOAA, USAID, and FEWSNET: Climate Prediction Center ' s Hispaniola Hazards Outlook For USAID / FEWS-NET Jult 11-July 17, 2013, Tech. rep., 2013.

OXFAM and Action contre la Faim: Etat des lieux de la situation de secheresse Dans les departements du Nord Ouest et du Haut Artibonite, Tech. rep., https://reliefweb.int/report/haiti/tat-des-lieux-de-la-situation-de-s-cheresse-dans-le-d-partement-du-nord-ouest-et-dans, 2015.

Palmer, W. C.: Keeping Track of Crop Moisture Conditions, Nationwide: The New Crop Moisture Index, Weatherwise, 21, 156–161, https://doi.org/10.1080/00431672.1968.9932814, 1968.

Peters, A. J., Walter-Shea, E. A., Ji, L., Vina, A., Hayes, M., and Svoboda, M. D.: Drought monitoring with NDVI-based Standardized Vegetation Index, Photogrammetric enginnering and remote sensing, 68, 71–75, 2002.

Sepulcre-Canto, G., Horion, S., Singleton, A., Carrao, H., and Vogt, J.: Development of a Combined Drought Indicator to detect agricultural drought in Europe, Natural Hazards and Earth System Sciences, 12, 3519–3531, https://doi.org/10.5194/nhess-12-3519-2012, 2012.

Serinaldi, F., Bonaccorso, B., Cancelliere, A., and Grimaldi, S.: Probabilistic characterization of drought properties through copulas, Physics and Chemistry of the Earth, 34, 596–605, https://doi.org/10.1016/j.pce.2008.09.004, http://dx.doi.org/10.1016/j.pce.2008.09.004, 2009.

Sheffield, J. and Wood, E. F.: Drought: past problems and future scenarios, Routledge, 2011.

Shiau, J.-T.: Fitting Drought Duration and Severity with Two-Dimensional Copulas, Water Resources Management, 20, 795–815, https://doi.org/10.1007/s11269-005-9008-9, 2006.

Shiau, J.-T., Feng, S., and Nadarajah, S.: Assessment of hydrological droughts for the Yellow River, China, using copulas, Hydrological Processes, 21, 2157–2163, 2007.

Songbai, S. and Singh, V. P.: Frequency analysis of droughts using the Plackett copula and parameter estimation by genetic algorithm, Stochastic Environmental Research and Risk Assessment, 24, 783–805, 2010.

Svoboda, M., Lecomte, D., Hayes, M., Heim, R., Gleason, K., Angel, J., Rippey, B., Tinker, R., Palecki, M., Stooksbury, D., Miskus, D., and Stephens, S.: The drought monitor, Bulletin of the American Meteorological Society, 83, 1181–1190, 2002.

Tadesse, T. and Wardlow, B. D.: The Vegetation Outlook (VegOut): A New Tool for Providing Outlooks of General Vegetation Conditions Using Data Mining Techniques, in: 7th IEEE International Conference on Data Mining Workshop, January, pp. 667–672, 2007.

Thornthwaite, C. and Mather, J.: The water balance, Climatology, 8, 1955.

Trading Economics: Haiti - Agricultural irrigated land (Percentage of total agricultural land), https://tradingeconomics.com/haiti/agricultural-irrigated-land-percent-of-total-agricultural-land-wb-data.html, 2013.

USAID and FEWSNET: HAITI Food Security Outlook Update June 2012, Tech. Rep. April, https://reliefweb.int/report/haiti/haiti-food-security-outlook-update-june-2012, 2012a.

USAID and FEWSNET: HAITI : Food Security Outlook Update March 2012, Tech. Rep. February, FEWSNET, http://fews.net/sites/default/files/documents/reports/Haiti{_}FSOU{_}2012{_}03{_}En{_}Final.pdf, 2012b.

USAID, MARNDR/CNSA, and FEWSNET: HAITI : Food Security Outlook Update June 2011, Tech. Rep. June, https://reliefweb.int/report/haiti/food-security-outlook-update-june-2011, 2011.

USDA Risk Management Agency, National Drought Mitigation Center, and University of Nebraska Lincoln: Weekly SPI, http://greenleaf.unl.edu/, 2006.

Wang, L. and Qu, J. J.: NMDI : A normalized multi-band drought index for monitoring soil and vegetation moisture with satellite remote sensing, Geophysical Research Letters, 34, 1–5, https://doi.org/10.1029/2007GL031021, 2007.

Wang, L., Li, X., Gong, J., and Song, C.: Vegetation temperature condition index and its application for drought monitoring, in: Geoscience and Remote Sensing Symposium, pp. 141–143, 2001.

Wilhite, D. A.: Drought as a natural hazard: Concepts and definitions, in: Drought: A Global Assessment, edited by Wilhite, D. A., chap. 1, pp. 3–18, Routledge, London, 2000.

World Bank: Haiti data, https://data.worldbank.org/country/haiti, 2017.

World Meteorological Organization: Standardized Precipitation Index User Guide, Tech. Rep. 1090, 2009.

World Meteorological Organization and Global Water Partnership: Handbook of Drought Indicators and Indices, 1173, https://doi.org/10.1201/9781315265551-12, www.droughtmanagement.info, 2016.

Zargar, A., Sadiq, R., Naser, B., and Khan, F. I.: A review of drought indices, Environmental Reviews, 19, 333–349, https://doi.org/10.1139/a11-013, 2011.

Zhu, J., Pollanen, M., Abdella, K., and Cater, B.: Modeling Drought Option Contracts, ISRN Applied Mathematics, 2012, 1–16, https://doi.org/10.5402/2012/251835, http://www.hindawi.com/isrn/appmath/2012/251835/, 2012.

Zhu, Y., Wang, W., Singh, V. P., and Liu, Y.: Combined use of meteorological drought indices at multi-time scales for improving hydrological drought detection, Science of the Total Environment, 571, 1058–1068, https://doi.org/10.1016/j.scitotenv.2016.07.096, http://dx.doi.org/10.1016/j.scitotenv.2016.07.096, 2016.

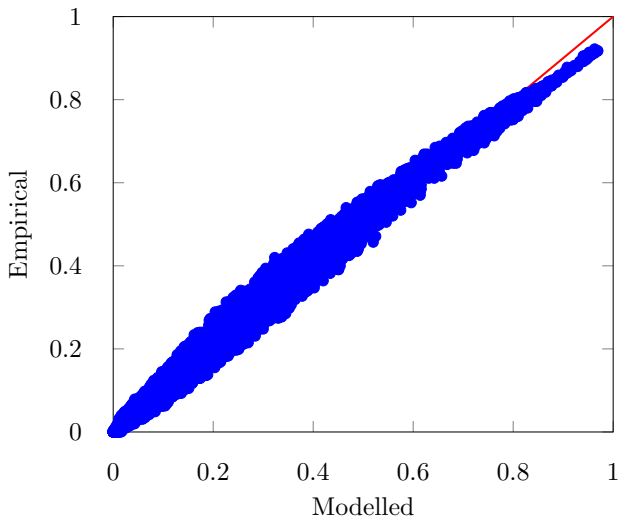

Figure 1. PPVI validation: empirical copula versus bivariate joint probability function. The red line corresponds to the 45°line. Joint probability values have been computed from Eq. 2, while empirical copula values according to Eq. 5.

Figure 2. Map of Haiti departments.

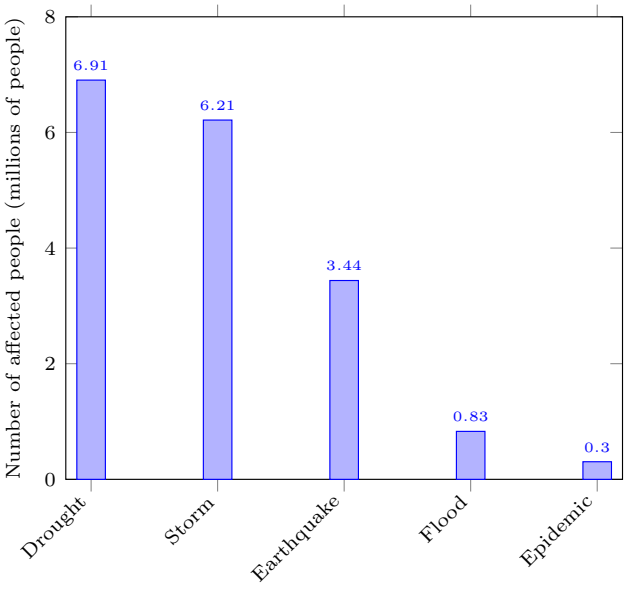

Figure 3. Number of people affected by natural disasters in Haiti (1900-2018). Source (CRED, 2017).

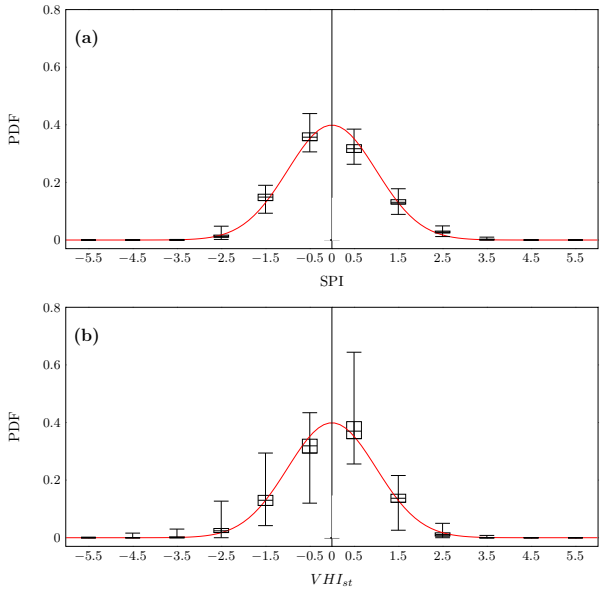

Figure 4. 4(a): distribution of SPI values; 4(b):distribution of VHI_{st} values. The red line represents the pdf of the standard normal distribution; boxplots represent the percentage of values lying in the range; 12 ranges were considered; starting from -6 and ending with 6 with a step equal to 1.

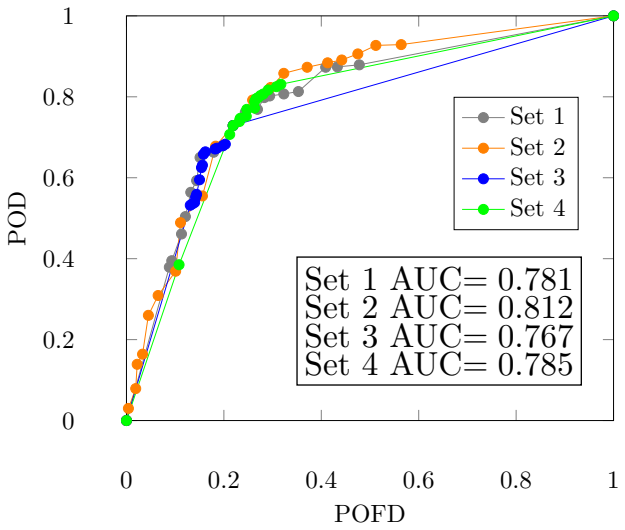

Figure 5. ROC curves for the set of thresholds reported in Table 9.

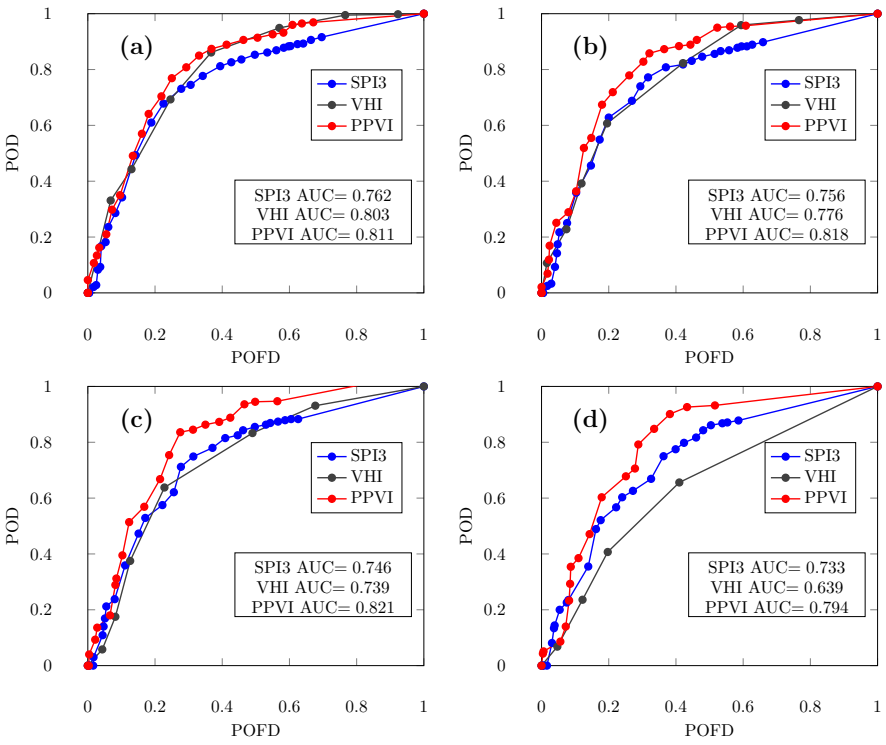

Figure 6. Comparison among the performances of SPI3, VHI and PPVI in identifying reported drought events; thresholds Z, Z_S and Z_V are varying, $z = -1.1$, $z_S = 0$ and $z_V = 40$; $n = 80$ and four cases for N are shown: (a): $N = 10\%$, (b): $N = 20\%$; (c):$N = 30\%$ and (d): $N = 50\%$.

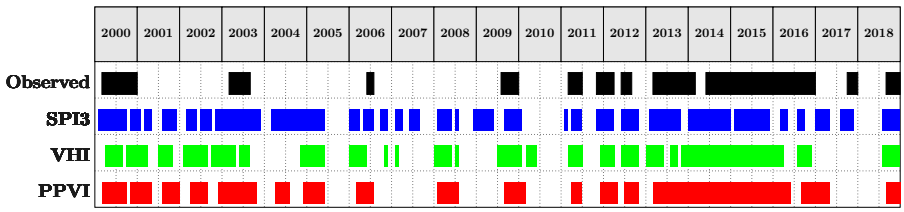

Figure 7. Comparison between observed drought events and drought events identified by PPVI, SPI3 and VHI when calibrated with the best performing parameters shown in Table 10. The comparison is shown for the period from 2000 to 2018

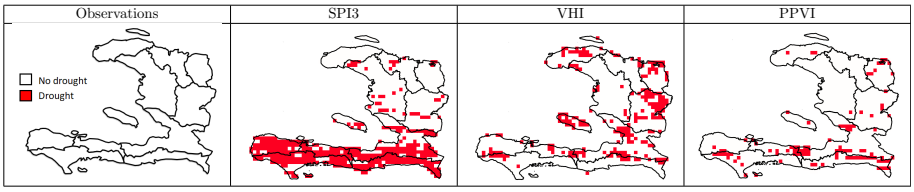

Figure 8. Comparison of the performance of SPI3, VHI, and PPVI in identifying the areas hit by drought. Week 45 of 1995. Departments highlighted in red are the ones in drought according to observations (Table 7), red cells are the ones in drought condition according to the various indices.

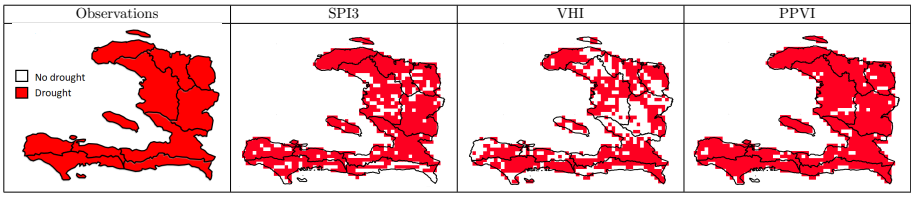

Figure 9. Same as Fig. 8 but for week 33 of 2015. Departments highlighted in red are the ones in drought according to observations, red cells are the ones in drought condition according to the various indices.

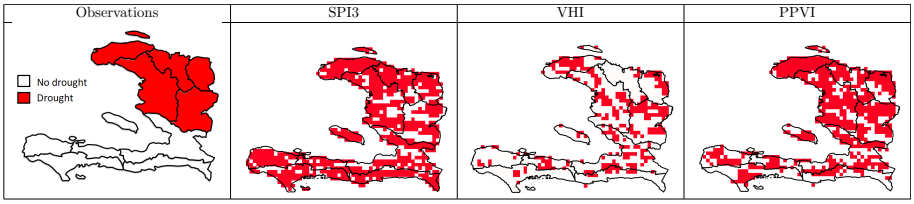

Figure 10. Same as Fig. 8 but for week 8 of 2012. Departments highlighted in red are the ones in drought according to observations, red cells are the ones in drought condition according to the various indices.

Table 1. An overview of indices used in agricultural drought monitoring; Met=Meteorological, Hydro=Hydrological, Ag=Agricultural.

Index	Inputs	Drought type	Pros	Cons	Reference
ETDI	Modeled (SWAT)	Ag	Analysis of both actual and potential ET	Complex calculations	(Narasimhan and Srinivasan, 2005)
NDVI	Near-infrared	Ag	High resolution, global coverage, remote-sensing	Need for data processing	(Kogan, 1995a)
SMAI	Precipitation, Temperature, Available water content	Ag	Water balance approach	Data requirements	(Bergman et al., 1988)
SMDI	Modeled (SWAT)	Ag	Adaptable to different crop types	Based upon output from SWAT	(Narasimhan and Srinivasan, 2005)
SSI	Soil moisture	Ag	Uses soil moisture only, standardized	Based on one variable	(Hao and Aghakouchak, 2013)
SVI	VCI	Ag	Standardized, remote-sensing	Scarcerly employed	(Peters et al., 2002)
SWS	Available Water content, Rooting depth, Soil water deficit, Soil type	Ag	Well known calculations	Poor performance on non-homogeneous soils	(BC Ministry for Agriculture, 2015)
TCI	Brightness temperature	Ag	High resolution, global coverage, remote-sensing	Only brightness temperature is considered	(Kogan, 1995a)
VCI	NDVI	Ag	High resolution, global coverage, remote-sensing	Identifies all vegetation stresses, not only the ones due to drought	(Liu and Kogan, 1996)
CMI	Precipitation, Temperature	Ag	Weekly temporal resolution	Specifically developed for grain-producing regions in the USA	(Palmer, 1968)

Table 1. Continued.

Index	Inputs	Drought type	Pros	Cons	Reference
CSDI	Precipitation, Temperature, wind speed, solar radiation, dewpoint temperature, soil profile, plant phenology	Ag	Very specific for each crop, based on plant development	Many inputs with a daily temporal resolution	(Meyer et al., 1993)
CWSI	Actual and potential evapotranspiration	Ag	Useful for irrigation scheduling, remote-sensing	To be computed from MODIS data	(Idso et al., 1981)
NMDI	NDVI	Ag	Uses vegetation condition and soil water content	Poor performance in areas with sparse vegetation	(Wang and Qu, 2007)
RSM	Precipitation, Temperature, Evapotranspiration, Soil properties, Crop features, Crop management practice	Ag	Computes the water balance with various methods	Need for multiple inputs	(Thornthwaite and Mather, 1955)
DTx	Modeled (water balance)	Ag	Computes an integrated transpiration deficit over a period of time	Need for multiple inputs	(Matera et al., 2007)
ADI	Precipitation, Snow water content, Streamflow, Reservoir storage, Evapotranspiration, Soil water content	Met Hydro Ag	Water balance approach	Need for multiple inputs	(Keyantash and Dracup, 2004)

Table 2. An overview of aggregate and composite drought indices useful for agricultural drought monitoring; Met=Meteorological, Hydro=Hydrological, Ag=Agricultural.

Index	Inputs	Drought type	Pros	Cons	Reference
VegDRI	SPI, NDVI, PDSI	Ag	Use of surface and remote-sensing data	Short period of record, Available only for the contiguous USA	(Brown et al., 2008)
VHI	VCI, TCI	Ag	High temporal resolution, global coverage at a high spatial resolution, 30+ years of records	Identifies all types of vegetation stress, not only the drought-related ones	(Kogan, 1990)
MSDI	SPI, SSI	Met Ag	Global coverage, remote-sensing	Grid size may not represent all areas and climate regimes equally well; short period of records	(Hao and Aghakouchak, 2013)
CDI	SPI3, fAPAR, SMA	Met Ag	10-day temporal resolution, high spatial resolution (5km)	Short period of record (2012), Available only in Europe, hard to replicate	(Sepulcre-Canto et al., 2012)
Morocco CDI	SPI, ET, LST, NDVI	Met Ag	High spatial resolution (5km)	Monthly temporal resolution; available for Morocco only, short period of record	(Bijaber et al., 2018)

Table 2. Continued.

Index	Inputs	Drought type	Pros	Cons	Reference
Hybrid DI	SPI, SWSI, PDSI	Met Hydro Ag	Function of damage, includes all types of droughts	Need for detailed information on economic damages	(Karamouz et al., 2009)
VegOut	SPI, NDVI, oceanic indices	Met Ag	Combination of climate information, vegetation condition, oceanic indices, and land cover	Need for a high number of parameters	(Tadesse and Wardlow, 2007)
OBDI	Precipitation, MPDI, Soil moisture	Met Ag	First attempt to combine and weight various inputs	Specifically designed for the USA	(Dieker et al., 2010)
USDM	PDSI, Soil moisture, Streamflow, Percent of normal precipitation, SPI, OBDI	Met Hydro Ag	Combines many inputs and expert knowledge, weekly temporal resolution	Available only for the USA	(Svoboda et al., 2002)
TVX	NDVI, LST	Ag	Combination of NDVI and temperature effects, remote-sensing	To be computed from NDVI and LST datasets	(Lambin and Ehrlich, 1995)
VTCI	NDVI, LST	Ag	Combination of NDVI and temperature effects, remote-sensing	To be computed from NDVI and LST datasets	(Wang et al., 2001)
AMDI-SA	MSPI, MSSI	Met Ag	Combination of SPI and SSI; standardized	Complex calculations	(Bateni et al., 2018)

Table 3. Drought classification based on SPI according to (Mckee et al., 1993).

Category	SPI	Probability (%)
Extremely wet	2.00 and above	2.3
Severely wet	1.50 to 1.99	4.4
Moderately wet	1.00 to 1.49	9.2
Near normal	-0.99 to 0.99	68.2
Moderately dry	-1.49 to -1.00	9.2
Severely dry	-1.50 to -1.99	4.4
Extremely dry	-2 and below	2.3

Table 4. Drought classification based on VHI according to (Dalezios et al., 2017).

Category	VHI
Extremely dry	≤ 10
Severely dry	≤ 20
Moderately dry	≤ 30
Mild dry	≤ 40
Normal	> 40

Table 5. Drought classification according to PPVI.

Category	PPVI	Probability (%)
Extremely wet	1.04 and above	2.3
Severely wet	0.58 to 1.03	4.4
Moderately wet	0.13 to 0.57	9.2
Near normal	-1.68 to 0.12	68.2
Moderately dry	-2.14 to -1.69	9.2
Severely dry	-2.15 to -2.59	4.4
Extremely dry	-2.6 and below	2.3

Table 6. Contingency table for the deterministic estimates of a series of binary events (Joliffe and Stephenson, 2012).

Events estimated	Events Observed Yes	No	Total
Yes	TP (True Positive or Hits)	FP (False Positive or False Alarms)	$TP + FP$
No	FN (False Negative or Missing)	TN (True Negative or Corret rejections)	$FN + TN$
Total	$TP + FN$	$FP + TN$	$TP + FP + FN + TN = T$

Table 7. Reported drought events in Haiti from 1980 to present.

Year	Department	Affected people	% population	Source
1981	South, Grand Anse, West	103'000	2	(Mora-Castro, 1986; CIAT, 2017)
1982-1983	South, South East, North West, North East	333'000	5.75	(Mora-Castro)
1984-1985	North West	13'500	2	(Mora-Castro, 1986; CIAT, 2017)
1986	All country			(Mora-Castro)
1990-1992	All country	1'000'000	14	(Mora-Castro)
1997	North West, North, North East	50'000	0.64	(CIAT, 2017)
2000	All country			(Mora-Castro)
2003	North West	35'000	0.41	(CIAT, 2017)
End 2009	North West			(CNSA/MARNDR and FEWSNET, 2009)
2011-2012	North, North West, North East, Artibonite, Centre			(USAID et al., 2011; USAID and FEWSNET, 2012a)
2013	All country	$> 143'000$	1.5	(NOAA et al., 2013; FEWSNET, 2013)
2014-2017	All country	3'600'000	33	(OXFAM and Action contre la Faim, 2015; NOAA, 2017)

Table 8. Number of significant correlations (Pearson correlation coefficient) between VHI and various SPI aggregation timescales. Value is expressed as percentage evaluated with respect to the total number of grid cells (987).

	% significant correlations 5%	% significant correlations 1%
SPI1	93.52	91.29
SPI2	96.76	95.34
SPI3	96.15	94.83
SPI6	90.07	85.82

Table 9. Example of set of thresholds used to draw ROC curves for model calibration. Thresholds N and n are expressed as the percentage of the country's area instead as the number of grid cells.

	Z	z	N	n	Step of variation
Set 1	-2	varying from -1.9 to 0	25%	10%	0.1
Set 2	varying from -3.5 to -1	-1	25%	10%	0.1
Set 3	-2	-1	25%	varying from 1% to 24%	1%
Set 4	-2	-1	varying from 11% to 25%	10%	1%

Table 10. Best configuration parameters for the model when applied with PPVI, SPI3 and VHI.

	Z	*z*	*N*	*n*	TN	FP	FN	TP	POFD	POD
PPVI	-1.8	-1.1	30%	8%	957	379	99	506	0.284	0.836
SPI3	-1.3	0	20%	8%	943	393	157	448	0.294	0.749
VHI	22	40	10%	8%	935	401	150	455	0.300	0.752

Table 11. Performance of PPVI, SPI3, and VHI in identifying departments hit by drought during week 8 of 2012 and comparison with observations. Observations are retrieved from the text-based documents reported in Table 7.

		% of the area			Ranking of affected departments		
Department	Reported as drought	PPVI	SPI3	VHI	PPVI	SPI3	VHI
North West	Yes	93.1	91.7	47.2	1	1	1
Artibonite	Yes	75.1	72.8	34.1	2	7	5
North	Yes	74.6	82.1	10.4	3	4	9
Centre	Yes	67.2	54.3	45.7	4	10	2
North East	Yes	62.1	72.4	34.5	5	8	4
West	No	61.8	72.1	32.7	6	9	6
Nippes	No	51.2	75.6	36.6	7	5	3
Grand Anse	No	47.8	82.1	10.4	8	3	8
South	No	32.6	75.3	9	9	6	10
South East	No	30.8	84.6	20	10	2	7

Table 12. Drought events in Haiti according to PPVI, duration, severity and mean areal extent.

Event number	Start date	End date	Duration (months)	Mean intensity PPVI	Minimum PPVI	Mean areal extent (%)
1	22/04/1982	21/07/1983	15	-8.46	-4.73	32.13
2	27/12/1984	07/11/1985	11	-7.87	-3.91	49.60
3	18/09/1986	16/04/1987	7	-7.90	-3.62	41.65
4	16/11/1989	18/10/1990	11	-8.60	-4.59	35.48
5	07/02/1991	11/02/1993	25	-8.70	-4.69	44.92
6	16/09/1993	27/01/1994	4	-8.95	-4.48	36.98
7	11/08/1994	10/11/1994	3	-8.53	-3.50	50.11
8	20/03/1997	20/11/1997	8	-8.43	-4.32	46.00
9	30/03/2000	21/09/2000	6	-8.31	-3.79	74.07
10	30/11/2000	19/04/2001	5	-7.98	-4.75	24.58
11	09/08/2001	06/12/2001	4	-7.85	-3.52	30.23
12	04/04/2002	08/08/2002	4	-8.25	-3.47	26.20
13	19/12/2002	30/10/2003	11	-7.72	-3.44	29.31
14	15/04/2004	22/07/2004	3	-7.69	-3.37	17.89
15	02/12/2004	26/05/2005	6	-9.00	-4.40	79.00
16	23/03/2006	13/07/2006	4	-7.46	-3.43	22.97
17	21/02/2008	31/07/2008	5	-7.95	-3.78	30.07
18	17/09/2009	18/02/2010	5	-8.58	-3.95	57.48
19	21/04/2011	16/06/2011	2	-9.32	-4.14	48.28
20	29/12/2011	05/04/2012	3	-8.12	-3.91	62.52
21	19/07/2012	25/10/2012	3	-8.33	-3.62	42.16
22	07/03/2013	05/05/2016	39	-8.18	-4.00	34.50
23	29/09/2016	20/04/2017	7	-8.20	-4.06	15.02
24	12/07/2018	31/12/2018	6	-9.50	-5.58	58.50